

RESEARCH ARTICLE

Open Access



tiRNA-Val promotes angiogenesis via Sirt1–Hif-1 α axis in mice with diabetic retinopathy

Yan Xu¹ , Haidong Zou^{1,2,3,4,5}, Qi Ding¹, Yuelan Zou¹, Chun Tang¹, Yuyu Lu¹ and Xun Xu^{1,2,3*}

Abstract

Background: Diabetic retinopathy (DR) is a specific microvascular complication arising from diabetes, and its pathogenesis is not completely understood. tRNA-derived stress-induced RNAs (tiRNAs), a new type of small noncoding RNA generated by specific cleavage of tRNAs, has become a promising target for several diseases. However, the regulatory function of tiRNAs in DR and its detailed mechanism remain unknown.

Results: Here, we analyzed the tiRNA profiles of normal and DR retinal tissues. The expression level of tiRNA-Val was significantly upregulated in DR retinal tissues. Consistently, tiRNA-Val was upregulated in human retinal microvascular endothelial cells (HRMECs) under high glucose conditions. The overexpression of tiRNA-Val enhanced cell proliferation and inhibited cell apoptosis in HRMECs, but the knockdown of tiRNA-Val decreased cell proliferation and promoted cell apoptosis. Mechanistically, tiRNA-Val, derived from mature tRNA-Val with Ang cleavage, decreased Sirt1 expression level by interacting with sirt1 3'UTR, leading to the accumulation of Hif-1 α , a key target for DR. In addition, subretinal injection of adeno-associated virus to knock down tiRNA-Val in DR mice ameliorated the symptoms of DR.

Conclusion: tiRNA-Val enhance cell proliferation and inhibited cell apoptosis via Sirt1/Hif-1 α pathway in HRMECs of DR retinal tissues.

Keywords: Diabetic retinopathy, tiRNAs, Sirt1, Hif-1 α

Background

Diabetic retinopathy (DR) is a common and a specific microvascular complication of diabetes [1], and it remains the leading cause of preventable blindness in working-aged people [2]. It has been reported that one-third of those people with diabetes have an increased risk of life-threatening systemic vascular complications, such as stroke, coronary heart disease, and heart failure [3, 4]. In the early events of DR, pronounced loss of pericytes and endothelial cells results in capillary occlusion and ischemia, and retinal ischemia/hypoxia leads to upregulation of VEGF through activation of hypoxia-inducible factor 1 (Hif-1) [5]. VEGF, a key factor involved

in the progression of proliferative diabetic retinopathy (PDR) and diabetic macular edema (DME), is believed to increase vascular permeability by inducing phosphorylation of tight junction proteins such as zonula occludens-1 (ZO-1) [6]. Additionally, endothelial cell adhesion molecules such as intercellular adhesion molecule-1 (ICAM-1), mediates leukocyte-endothelium adhesion in DR, are found to be increased in DR animals and patients [7]. However, the pathogenesis of the onset of DR disease is not completely understood as of yet.

Noncoding RNAs (ncRNAs) have emerged as critical regulators of various biological processes in DR, such as cell proliferation, cell motility, immune and inflammatory responses [8]. For example, the expression of MIAT, a long noncoding RNA (lncRNA), increased in diabetic retinas, while MIAT knockdown ameliorated diabetes mellitus-induced retinal microvascular dysfunction [9]. miRNA-138-5p is expressed at low levels in the retinal

*Correspondence: drxuxun@sjtu.edu.cn

¹ Shanghai Eye Diseases Prevention & Treatment Center/ Shanghai Eye Hospital, Shanghai, China

Full list of author information is available at the end of the article



© The Author(s) 2022. **Open Access** This article is licensed under a Creative Commons Attribution 4.0 International License, which permits use, sharing, adaptation, distribution and reproduction in any medium or format, as long as you give appropriate credit to the original author(s) and the source, provide a link to the Creative Commons licence, and indicate if changes were made. The images or other third party material in this article are included in the article's Creative Commons licence, unless indicated otherwise in a credit line to the material. If material is not included in the article's Creative Commons licence and your intended use is not permitted by statutory regulation or exceeds the permitted use, you will need to obtain permission directly from the copyright holder. To view a copy of this licence, visit <http://creativecommons.org/licenses/by/4.0/>. The Creative Commons Public Domain Dedication waiver (<http://creativecommons.org/publicdomain/zero/1.0/>) applies to the data made available in this article, unless otherwise stated in a credit line to the data.

tissues of DR rats and it regulates early DR by promoting cell proliferation by targeting NOVA1 [10]. Recently, tRNA cleavage products have been identified as functional noncoding RNAs, called tRNA-derived stress-induced RNAs (tiRNAs), tRNA-derived RNA fragments (tRFs), or tRNA-derived small RNAs (tsRNAs) [11–13]. tiRNAs are generated by specific cleavage in the anticodon loops of mature tRNAs or pre-tRNAs and are 31–40 bases long [14]. The expression pattern of tiRNAs does not correspond to cognate tRNA levels, demonstrating that tiRNAs are not degradation products and precisely regulate noncoding RNAs [15]. tiRNAs are an emerging class of regulatory non-coding RNAs that play important roles in regulating a variety of biological processes, such as competition for ribosomes [16], destabilizing YBX1-Bound mRNAs [17], and target mRNAs [18]. However, the role of tiRNAs in DR is yet to be elucidated (Additional file 1: Fig. S1).

In this study, we constructed a DR mouse model with STZ-induced diabetes to analyze tiRNA profile of normal and DR retinal tissues. The expression level of tiRNA-Val was significantly upregulated in DR retinal tissues and in human retinal microvascular endothelial cells (HRMECs) under high glucose condition. tiRNA-Val enhanced cell proliferation and inhibited apoptosis in HRMECs. In addition, tiRNA-Val, derived from mature tRNA-Val, decreased Sirt1 expression level by interacting with Sirt1 3'UTR, leading to the accumulation of Hif-1 α . Moreover, the knockdown of tiRNA-Val in retinal tissues drastically ameliorated the symptoms of DR in vivo. tiRNA-Val gene may be a potential target for diabetic retinopathy.

Materials and methods

Cell lines and cell culture

HRMECs were purchased from American type culture collection (ATCC). HRMECs were cultured in Dulbecco's modified eagle's medium (DMEM) (Sigma-Aldrich, USA) supplemented with 1% penicillin/streptomycin (100 mg/L, Gibco, USA) and 10% heat-inactivated fetal bovine serum (FBS) (Gibco, USA) at 37 °C in 5% CO₂ atmosphere. For normal glucose and high glucose conditions, 5 mM and 33 mM D-glucose (Gibco, USA) were added to the medium for 48 h, respectively.

Animals

All animal experiments were approved by the Institutional Animal Care and Use Committee of Shanghai General Hospital and were performed in accordance with the ARVO Statement for the Use of Animals in Ophthalmic and Vision Research. C57BL/6 male mice were purchased from Shanghai Model Organisms Center. The animals were housed in cages with free access to regular diet and water in a room at 22 \pm 1 °C on a 12 h light/

dark cycle. When the mice reached 20–25 g body weight (~2 months of age), they were randomly assigned into diabetic or nondiabetic group. Diabetes was induced by five sequential daily intraperitoneal injections of a freshly prepared solution of streptozotocin in citrate buffer (pH 4.5) at 45 mg/kg body weight. Mice with random blood glucose levels \geq 16.7 mmol/L at 2 weeks post-STZ were assigned to the diabetes group and the diabetes duration commenced. The animals had free access to food and water. Retinal tissues were harvested at 9 months of diabetes for protein extraction, RNA extraction, and retinal histopathology. Fasting blood glucose levels were determined repeatedly prior to the 3-month assessment.

For subretinal injection, adeno-associated virus (AAV) vector containing sh-tiRNA-Val under the control of chimeric CMV/chicken β -actin promoter was constructed. The vectors were administered via subretinal injection two weeks before STZ induction of diabetes. C57BL/6 male mice were anesthetized and subretinally injected with 1 μ L solution containing 10¹¹ particles of sh-tiRNA-Val AAV, as previously described [19]. The solution was injected only in one eye for each animal, while the contralateral eye was used as a control. Retinal tissues were harvested after 9 months of diabetes.

Cell transfection

tiRNA-Val mimics, tiRNA-Val inhibitors, and corresponding negative controls were purchased from Sangon Biotech (Shanghai, China). Lipofectamine 3000 transfection reagent (Invitrogen, USA) was used for cell transfection according to the manufacturer's instructions. The final concentrations of tiRNA-Val mimics and tiRNA-Val inhibitors were 50 nM, respectively.

Cell proliferation assay

Cell viability was assessed using CCK-8 assay (Cell Counting Kit-8, Sigma-Aldrich, USA) according to the manufacturer's instructions. Briefly, 5 \times 10³ cells/well were seeded into 96-well plates. Proliferative activity was determined at the end of different experimental periods (24 h, 48 h, 72 h, and 96 h). When the medium changed from red to yellow, the absorbance value at a wavelength of 450 nm was detected using an enzyme-linked immunosorbent assay reader (Thermo Fisher Scientific, USA). The experiment was performed at least three times with similar results.

Transwell migration assay

The migratory ability of HRMECs was assessed using 24-well transwell migration chambers (8 μ m size, Corning, USA). Briefly, 5 \times 10⁴ cells/well were resuspended in 200 μ L serum-free DMEM and inoculated evenly into the inner chambers. The bottom chambers were replenished

with 500 μ L of DMEM containing 20% FBS as an attractant. After 24 h, the cells migrated to the lower chamber through the hole, fixed with 4% paraformaldehyde, and then stained with 0.1% crystal violet.

Western blotting

Cell lysates or mouse tissues were prepared using $1 \times$ cell lysis buffer (Cell Signaling Technology, USA) with 1 mM phenylmethylsulfonyl fluoride (PMSF; Sigma-Aldrich, USA). Protein lysate of 10–20 μ g was run on 10–15% SDS-PAGE gel and transferred to a PVDF membrane (Roche, USA). The membrane was incubated for 60 min at room temperature in 5% BSA solution. The following antibodies were used for the detection of protein expression: actin (1:1,000, Sigma, USA), angiogenin (Ang) (1:1,000, Abcam, USA), VEGF (1:1,000, Thermo Fisher Scientific, USA), ZO-1 (1:1,000, Thermo Fisher Scientific, USA), ICAM-1 (1:1,000, Abcam, USA), Sirt1 (1:1,000, Cell Signaling Technology, USA), and Hif-1 α (1:1,000, Cell Signaling Technology, USA). Anti-rabbit and anti-mouse peroxidase-conjugated secondary antibodies (1:2,000, Cell Signaling Technology, USA) were purchased from Jackson ImmunoResearch, and the signal was visualized using western blotting luminol reagent (Thermo Fisher Scientific, USA).

Quantification of mRNA by RT-qPCR

Total RNA was isolated from cultured cells or mouse tissues using TRIzol reagent (Thermo Fisher Scientific, USA) according to the manufacturer's instructions. For mRNA quantification, cDNA was synthesized using SuperScript IV Reverse Transcriptase (Thermo Fisher Scientific, USA) with random primers. RT-qPCR was performed using SYBR Green method. The primers used for amplification are listed in Additional file 2: Table S1, and each experiment was repeated at least three times independently. The mRNA expression levels were calculated using β -actin as an internal control.

Quantification of tiRNA by TaqMan RT-qPCR

TaqMan RT-qPCR for specific quantification of tiRNA was performed as previously described. Briefly, total RNA was treated with T4 PNK (New England Biolabs, UK), followed by ligation to 3'-RNA adapter using T4 RNA ligase. Ligated RNA was then subjected to TaqMan RT-qPCR using SuperScript IV Reverse Transcriptase, 200 nM of TaqMan probe targeting the boundary of target RNA and 3'-adapter, and specific forward and reverse primers. The expression of tiRNA was calculated using 5S RNA as an internal control. The sequences of the TaqMan probes and primers are listed in Additional file 2: Table S2.

RNA cleavage reaction in vitro

RNA cleavage was performed as previously described [20]. Briefly, the incubation mixtures contained 20 μ g of total RNA extracted from HRMEC, 30 mM HEPES, pH 6.8, 30 mM NaCl, 0.001% BSA, and recombinant human angiogenin protein (R&D Systems, USA) at concentrations of 0.1 μ M, 0.2 μ M, 0.5 μ M, 1.0 μ M, and 2.0 μ M. Incubation was performed at 37 °C for 30 min. The cleaved products were recovered through phenol–chloroform extraction and ethanol precipitation. Then, the products were analyzed through northern blotting.

Northern blotting

Northern blotting for specific detection of small RNA was performed as previously described [21]. Briefly, total RNA was separated using 15% urea PAGE. Gels were stained with SYBR Gold nucleic acid gel stain (Thermo Fisher Scientific, USA) and immediately imaged and transferred to positively charged nylon membranes (Roche, Switzerland). Subsequently, the membranes were air-dried and UV-crosslinked. The membranes were pre-hybridized with DIG Easy Hyb buffer (Roche, Switzerland) for at least 1 h at 45 °C. For the detection of specific small RNAs, the membranes were incubated overnight at 45 °C with 10 nM 3'-DIG-labeled oligonucleotide probes synthesized by Sangon Biotech (Shanghai, China), as shown in Additional file 2: Table S3. The membranes were washed twice with low stringent buffer (2 \times SSC with 0.1% (w/v) SDS) at 37 °C for 15 min each, then rinsed twice with high stringent buffer (0.1 \times SSC with 0.1% (w/v) SDS) at 37 °C for 5 min each, and finally rinsed in washing buffer (1 \times SSC) for 10 min. Following the washes, the membranes were transferred onto 1 \times blocking buffer (Roche) and incubated at room temperature for 2–3 h, after which DIG antibody (Roche) was added to the blocking buffer at a ratio of 1:10,000 and incubated for an additional 1/2 min at room temperature. The membranes were then washed four times in DIG washing buffer (1 \times maleic acid buffer, 0.3% Tween-20) for 15 min each, rinsed in DIG detection buffer (0.1 M Tris-HCl, 0.1 M NaCl, pH 9.5) for 5 min, and then coated with CSPD ready-to-use reagent (Roche, Switzerland). The membranes were incubated in the dark with CSPD reagent for 15 min at 37 °C before imaging using the Carestream imaging system.

Luciferase assay

HEK293T cells in a 24-well plate were co-transfected with pSIF-GFP or the indicated plasmids expressing tiRNA (0.8 μ g/well), pRL-Sirt1-3' UTR (pRL-TK vector containing Sirt1 3'UTR) or pRLSirt1-3'UTRm (pRL-TK vector containing mutant Sirt1 3'UTR) (0.1 μ g/well), and

pSV40- β -gal (Promega, Madison, WI, USA) (0.1 μ g/well) using lipofectamine 3000. HRMEC cells in a 24-well plate were co-transfected with the indicated tiRNA mimics, pRL-Sirt1-3'UTR (0.1 μ g/well), and pSV40- β -gal (0.1 μ g/well) using lipofectamine 3000. After transfection for 72 h, the cells were harvested for luciferase assay as previously described [20].

Statistical analysis

Quantitative data are represented as mean \pm SD. All images are representative of the studies with three to nine animals per group. Paired Student's *t*-test was used to assess the significant difference between the two groups. Statistical significance was set at $p \leq 0.05$.

Results

tiRNA profile in DR retinal tissues from mice

We constructed a mouse model with diabetic retinopathy according to a previously described method [22]. The average fasting blood glucose level in DR mice was 19.0 mmol/L, which is far higher than that in normal mice (4.8 mmol/L) (Fig. 1a). The mRNA expression levels of VEGF and ICAM-1 were significantly upregulated in DR retinal tissues, while the mRNA expression level of ZO-1 was significantly downregulated (Fig. 1b). The protein levels of VEGF, ICAM-1, and ZO-1 also changed based on the mRNA level (Fig. 1c, d). To evaluate the degeneration of retinal neurons, we examined retinal ganglion cell layer (GCL) after 9 months of diabetes. Diabetic mice experienced 10% loss of neurons in retinal GCL compared to that in non-diabetic mice (Fig. 1e).

To explore the physiological relevance of tiRNAs, TaqMan RT-qPCR quantification of all the tiRNAs that cleaved at the anticodon loop was performed for DR retinal tissues of mice. As shown in Fig. 1e, the tiRNA profile was significantly altered in the retinal tissues of DR mice, especially tiRNA-Val, which was markedly upregulated. Therefore, we chose tiRNA-Val as a candidate for this study.

tiRNA-Val was derived from mature tRNA-Val, which was cleaved at the anticodon loop with RNase (Fig. 1g). We analyzed the expression level of tiRNA-Val through northern blotting. As shown in Fig. 1h, no significant

differences were observed in the expression level of mature total tRNA-Val, but tiRNA-Val was significantly upregulated in the retinal tissues of DR mice.

tiRNA-Val was upregulated in HRMEC at high glucose condition

Furthermore, HRMECs treated with the indicated concentrations of glucose were used to simulate various diabetic conditions [23]. HRMECs were cultured under normal glucose (5 mM) or high-glucose (33 mM) conditions. The mRNA and protein levels of VEGF, ICAM-1, and ZO-1 significantly changed in HRMEC at high glucose condition (Fig. 2a–c), and the expression level of tiRNA-Val was upregulated in HRMECs under high glucose conditions (Fig. 2d and e).

tiRNA-Val enhance cell proliferation in HRMEC

DR is a proliferative manifestation of the retina accompanied by the growth of abnormal new blood vessels [24]. We investigated the regulatory function of tiRNA-Val in cell proliferation by performing tiRNA-Val transfection. In view of the high expression of tiRNA-Val in the retinal tissues of DR mice and high glucose cell models, we examined the effect of tiRNA-Val on proliferation and migration of HRMECs. tiRNA-Val mimics and tiRNA-Val inhibitors were transfected into HRMECs, respectively (Fig. 3a), followed by CCK-8 (Fig. 3b) and Transwell migration assays (Fig. 3c). As shown in Fig. 3b, the viability of HRMECs increased markedly by transfection with tiRNA-Val mimics, and the enhanced effect of tiRNA-Val mimics on cell proliferation was observed beginning at 48 h. HRMECs transfected with tiRNA-Val mimics migrated significantly faster than those in the cells transfected with the negative control (Fig. 3c, d). To further investigate the effect of tiRNA-Val on cell apoptosis in HRMECs, FITC Annexin V apoptosis detection was performed. It was found that cells transfected with tiRNA-Val mimics could significantly inhibit cell apoptosis compared to that in cells transfected with the negative control (Fig. 3e). In addition, HRMECs transfected with tiRNA-Val inhibitors to knock down tiRNA-Val decreased cell proliferation (Fig. 3b) and migration (Fig. 3c and d), but promoted cell apoptosis (Fig. 3e).

(See figure on next page.)

Fig. 1 tiRNA profile between normal and DR retinal tissues in mice. **a** Blood glucose level in normal and DR mice. Data are represented as the mean \pm SD, $n = 9$, $***p < 0.001$ vs. normal group. Statistical significance was assessed by two-tailed Student's *t*-test. **b** qRT-PCR analysis of VEGF, ICAM-1, and ZO-1 levels in the entire retina of DR mice. Data are represented as the mean \pm SD, $n = 6$, $***p < 0.001$ vs. normal group. Statistical significance was assessed by two-tailed Student's *t*-test. **c, d** Western blotting analysis of VEGF, ICAM-1, and ZO-1 expression in the entire retina of normal and DR mice. Data are represented as the mean \pm SD, $n = 3$, $***p < 0.001$ vs. Control group. Statistical significance was assessed by two-tailed Student's *t*-test. **e** Representative micrographs of H&E staining of the retina tissue in mice treated as indicated. Scale bar, 210 μ m. **f** Heatmap of differently expressed tiRNAs between normal and DR mice retinal tissues by TaqMan RT-qPCR. **g** Structure of tiRNA-Val and total tRNA-Val. (h) Expression level of tiRNA-Val identified in five pairs of normal and DR retinal tissues by northern blot. GCL: ganglion cell layer; IPL: inner plexiform layer; INL: inner nuclear layer; OPL: outer plexiform layer; ONL: outer nuclear layer; PR: photoreceptors; RPE: retinal pigment epithelium; DR: diabetic retinopathy

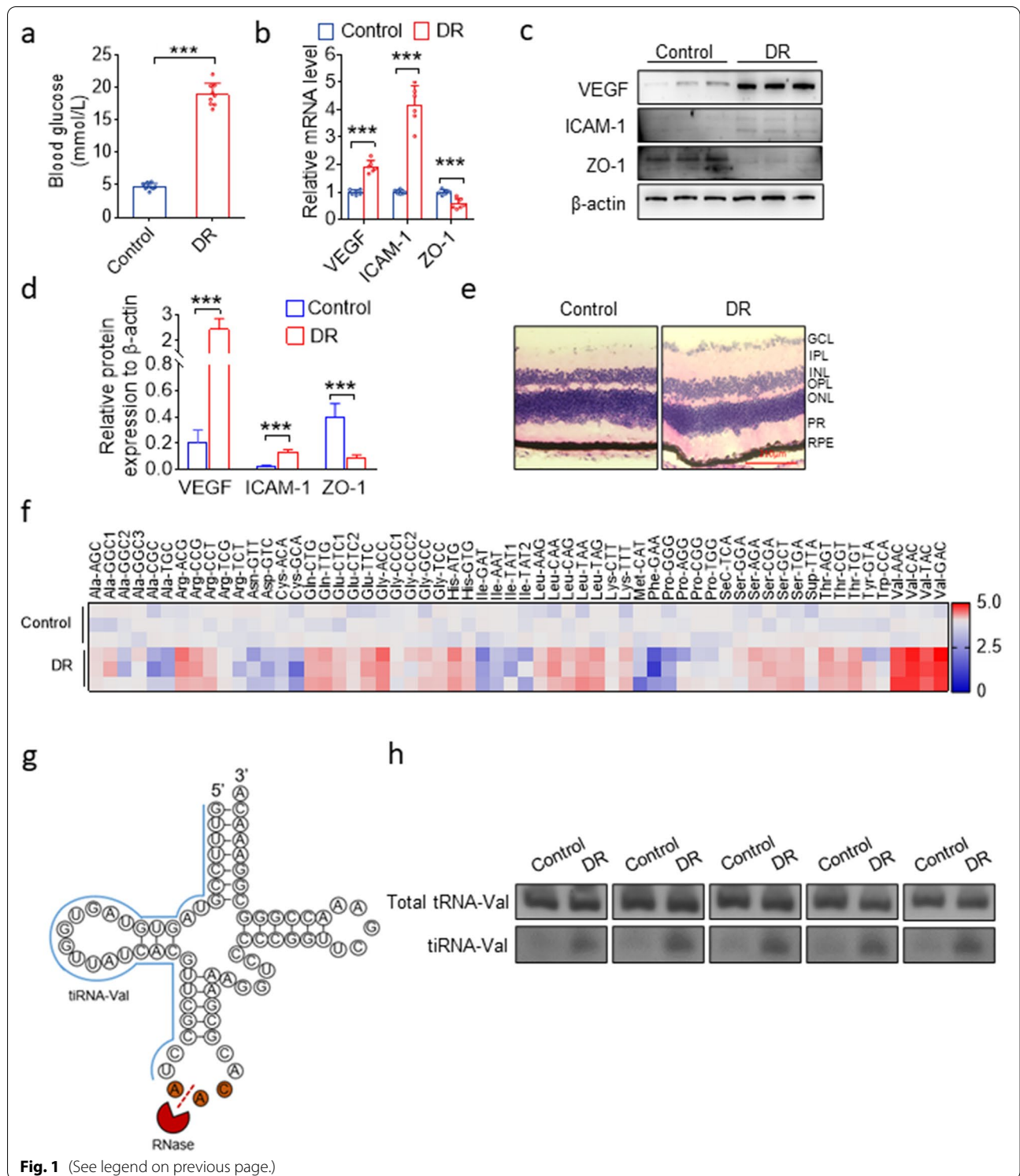
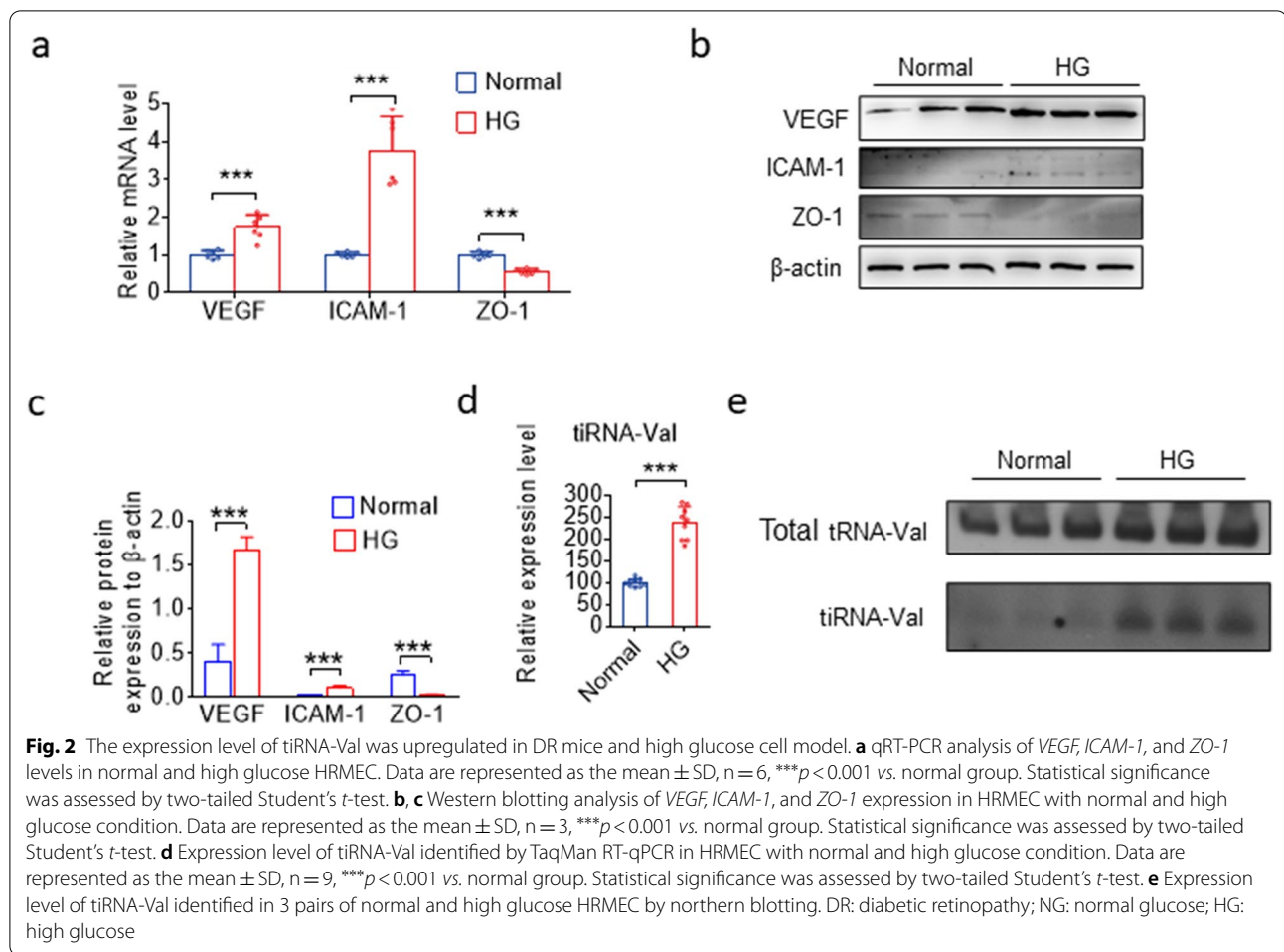


Fig. 1 (See legend on previous page.)

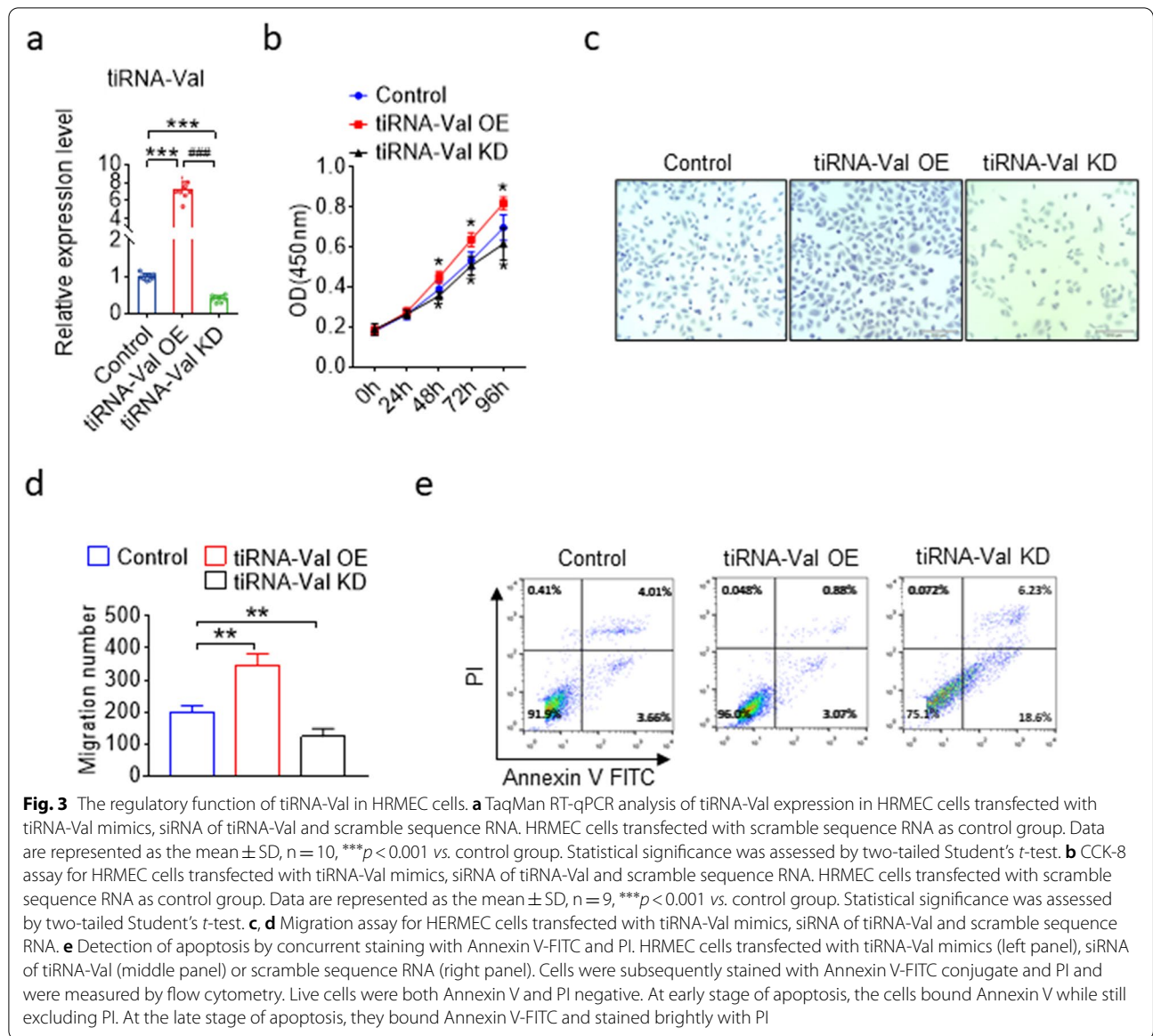


Ang cleaves tRNA-Val to produce tiRNA-Val in mouse retinal tissues and HRMEC cell models

Previous studies have shown that tiRNA production is dependent on Ang, which is the fifth member of the RNase A superfamily [20, 25]. The mRNA and protein levels significantly increased in the retinal tissues of DR mice (Fig. 4a and b). To test whether Ang could cleave tRNA-Val, total RNA from HRMECs was incubated with recombinant Ang in vitro. Northern blotting results showed that intact tRNA-Val was cleaved into short tRNA fragments of the length of tiRNA-Val (Fig. 4c). To test whether Ang could cleave tRNAs in cultured mammalian cells, HRMECs were transiently transfected with a plasmid expressing angiogenin. Total cellular RNA was extracted after transfection for 48 h. tiRNA-Val significantly increased in Ang-overexpressing cells (Fig. 4d, e). However, tiRNA-Val levels were not detected in HRMECs transfected with Ang siRNA (Fig. 4f, g). These results suggest that Ang is possibly an endonuclease for producing tiRNA-Val in vivo.

tiRNA-Val increased Hif-1 α expression level by interacting with Sirt1 3'UTR

tiRNAs are a new class of small RNAs with different mechanisms to regulate various cellular processes [15]. Hif-1 α is a key mediator and target of retinal neovascularization and diabetic retinopathy [26, 27], and during hypoxia, Sirtuin 1 (Sirt1) is downregulated, which allows the acetylation and activation of Hif-1 α . We found that tiRNA-Val could pair with the 3'UTR of Sirt1 (Fig. 5a). Then, a luciferase reporter under the control of Sirt1 3'UTR was used to examine the effect of tiRNA-Val. As shown in Fig. 5b, the overexpression of tiRNA-Val significantly downregulated the activity of Sirt1 3'UTR, whereas the overexpression of tiRNA-Val had no effect on the mutant reporter. To further confirm whether tiRNA-Val targets Sirt1 3'UTR, a plasmid expressing mutant tiRNA-Val with ten mismatched bases was constructed, and we found that the mutant tiRNA-Val had no effect on the activity of Sirt1 3'UTR (Fig. 5c). To further examine the relationship among tiRNA-Val, Hif-1 α ,



and Sirt1, we performed transfection with tiRNA-Val mimics and found that Hif-1 α protein levels significantly increased, whereas Sirt1 protein levels decreased (Fig. 5d, e). Similarly, Hif-1 α protein level was upregulated, but the protein level of Sirt1 significantly decreased in the retinal tissue of DR mice (Fig. 5f, g). These data demonstrate that tiRNA-Val decreased Sirt1 expression level by interacting with Sirt1 3'UTR leading to the accumulation of Hif-1 α .

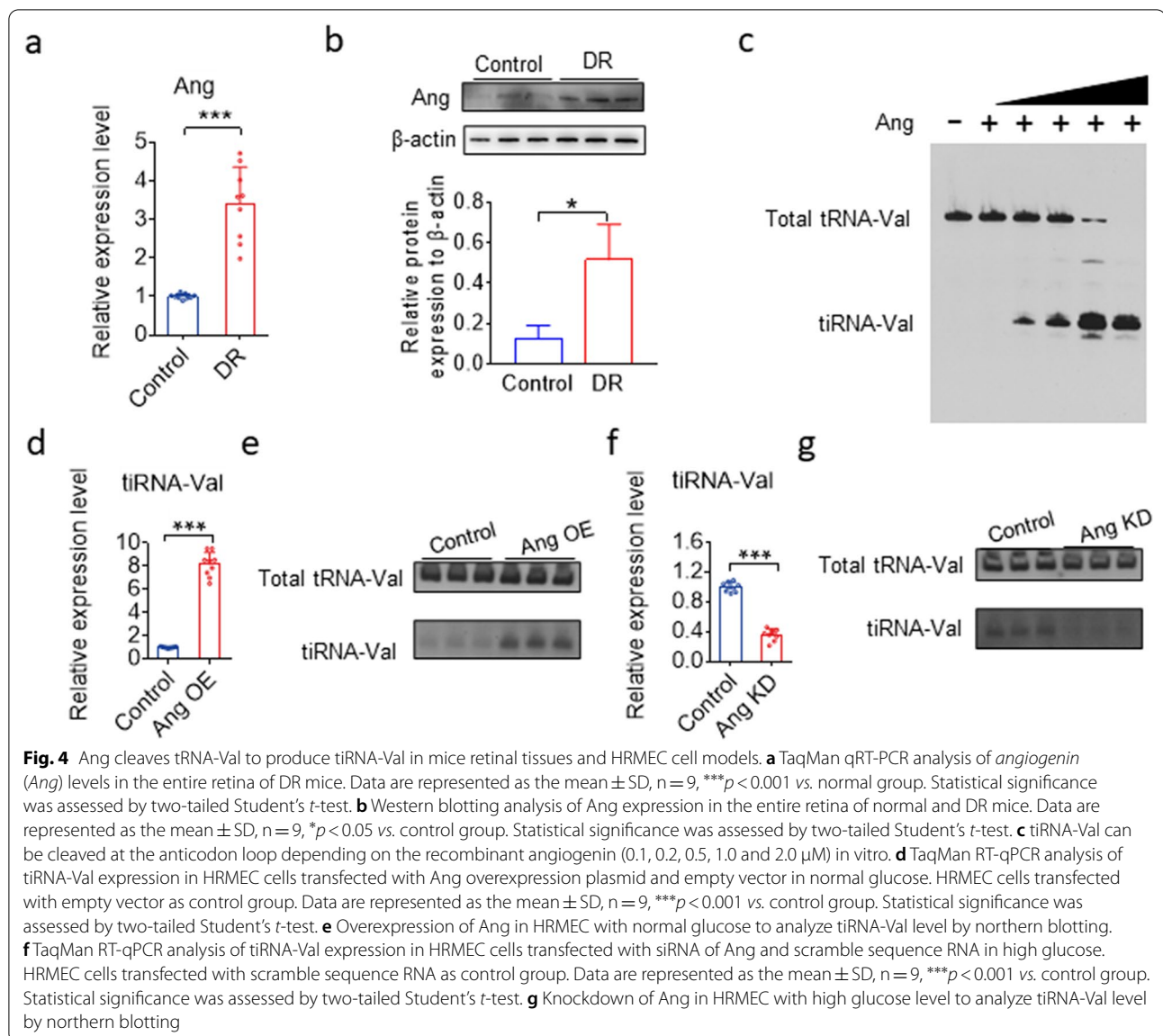
Knockdown of tiRNA-Val ameliorates DR in vivo

To explore tiRNA in vivo, we knocked down tiRNA-Val in the subretinal space of DR mice with AAV -shtiRNA-Val. As shown in Fig. 6a and b, the expression level of tiRNA-Val

decreased to 34.9%. The protein level of Sirt1 significantly increased when tiRNA-Val was knocked down, and Hif-1 α was downregulated (Fig. 6c, d). Importantly, the mRNA and protein levels of VEGF and ICAM-1 were downregulated, while ZO-1 increased significantly (Fig. 6e–g). Moreover, the loss of neurons in GCL was recovered compared to that in diabetic mice with control AAV (Fig. 6h). These data demonstrated that the knockdown of tiRNA-Val ameliorated the symptoms of DR in vivo.

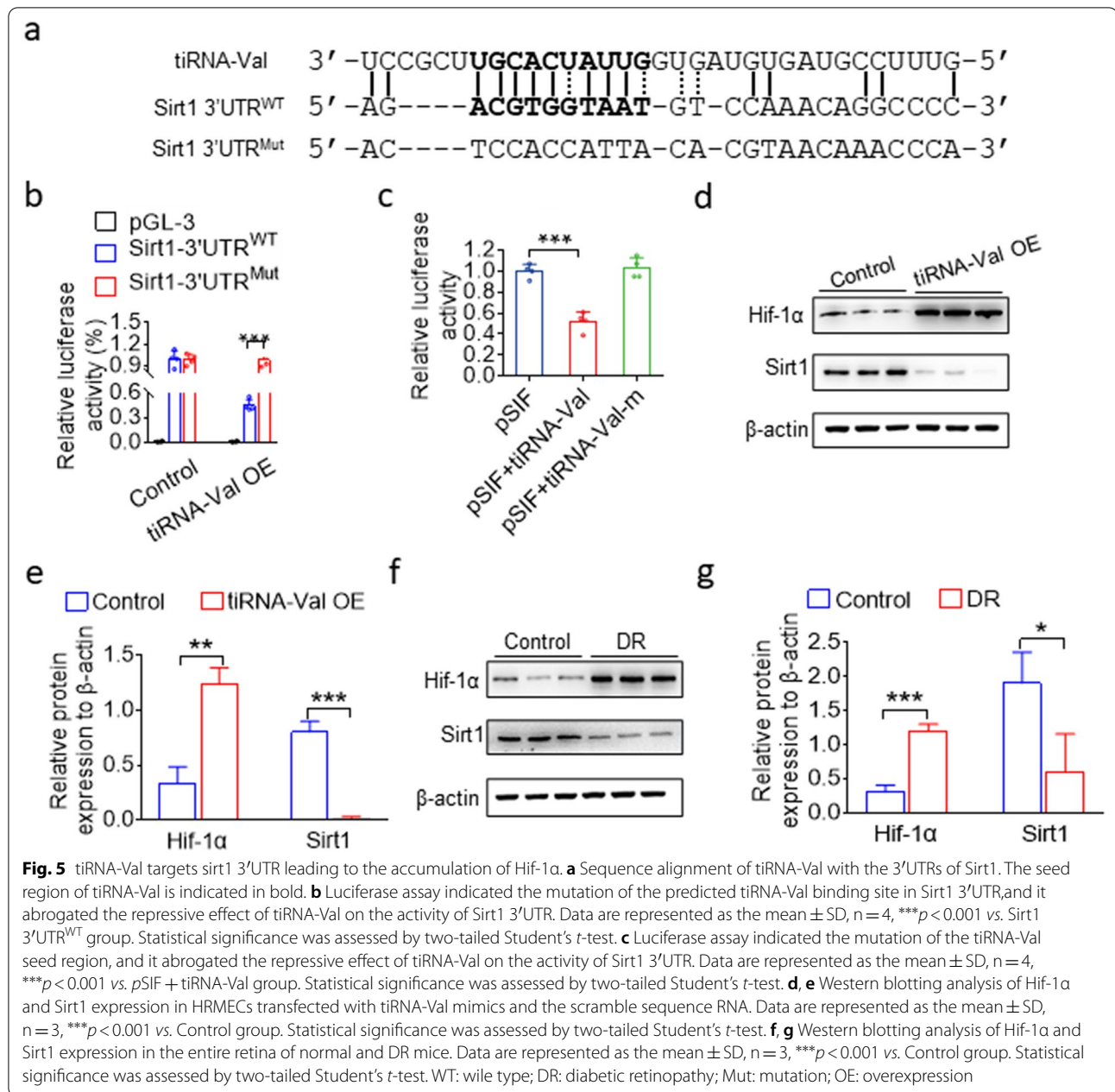
Discussion

In this study, we found that tRNA-derived small RNA, tiRNA-Val, was upregulated in the retinal tissues of DR mice. Ang, a member of the RNase A family, cleaved



mature tRNA-Val to tiRNA-Val, which could enhance cell proliferation in HRMECs. Furthermore, we identified Sirt1 as the direct target of tiRNA-Val and demonstrated that tiRNA-Val negatively regulated Sirt1 in DR. It has been reported that hypoxia decreases Sirt1 expression, leading to the acetylation and activation of Hif-1 α [28]. Our findings showed that tiRNA-Val downregulated the expression level of Sirt1, leading to the accumulation of Hif-1 α . The knockdown of tiRNA-Val in the subretinal space ameliorated DR via Sirt1-Hif-1 α axis in vivo (Fig. 7). These results suggest that tiRNA-Val may represent a potential therapeutic target for the treatment of DR.

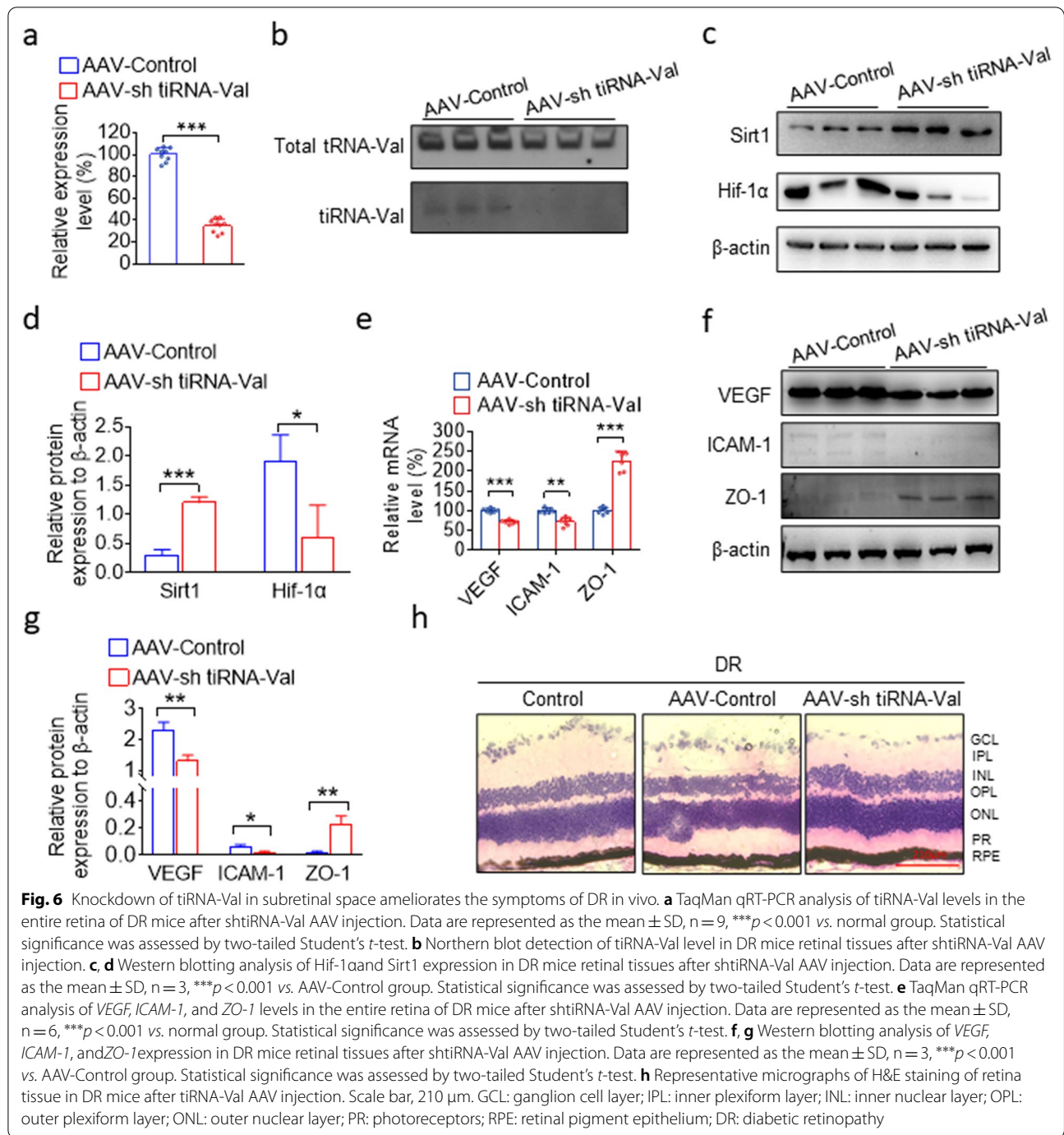
High-throughput sequencing has resulted in the discovery of a new class of small RNAs: tRFs and tiRNAs derived from tRNAs. tiRNAs are activated under stress conditions and they modulate the stress response [29]. Although they are named stress fragments, they are detected under non-stressed conditions [30]. tiRNAs span the entire evolutionary tree, and biological roles have been identified for some tiRNAs in subsets of organisms. For example, tiRNA-Ala can inhibit protein synthesis and promote stress granule formation in a phospho eIF2 α independent manner, inhibiting translation by displacing the eukaryotic initiation factor eIF4G/A from mRNAs [25]. A group of tiRNAs



competitively bind to cytochrome c, protecting cells from apoptosis during osmotic stress cytochrome c [31]. tiRNAs from the sperm contribute to intergenerational inheritance and alter the expression profile and RNA modifications of many genes [32]. Here, we found that tiRNA-Val negatively regulated Sirt1 in DR by interacting with Sirt1 3'UTR. Previous studies have shown that tRNA-derived fragments can repress endogenous genes to regulate cell proliferation and modulate DNA damage response [33, 34]. It is possible

that tiRNAs play a key role in regulating gene expression levels in miRNA pathway or take part in other mechanisms.

SIRT1 is a nicotinamide adenosine dinucleotide (NAD)-dependent multifunctional deacetylase that removes acetyl groups from many proteins that can be implicated in diabetes [35]. It was reported that Sirt1 was downregulated in DR patients [36]. Sirt1 regulated the expression of Hif-1α, especially under hypoxic condition; thus, it was involved in multiple biological processes



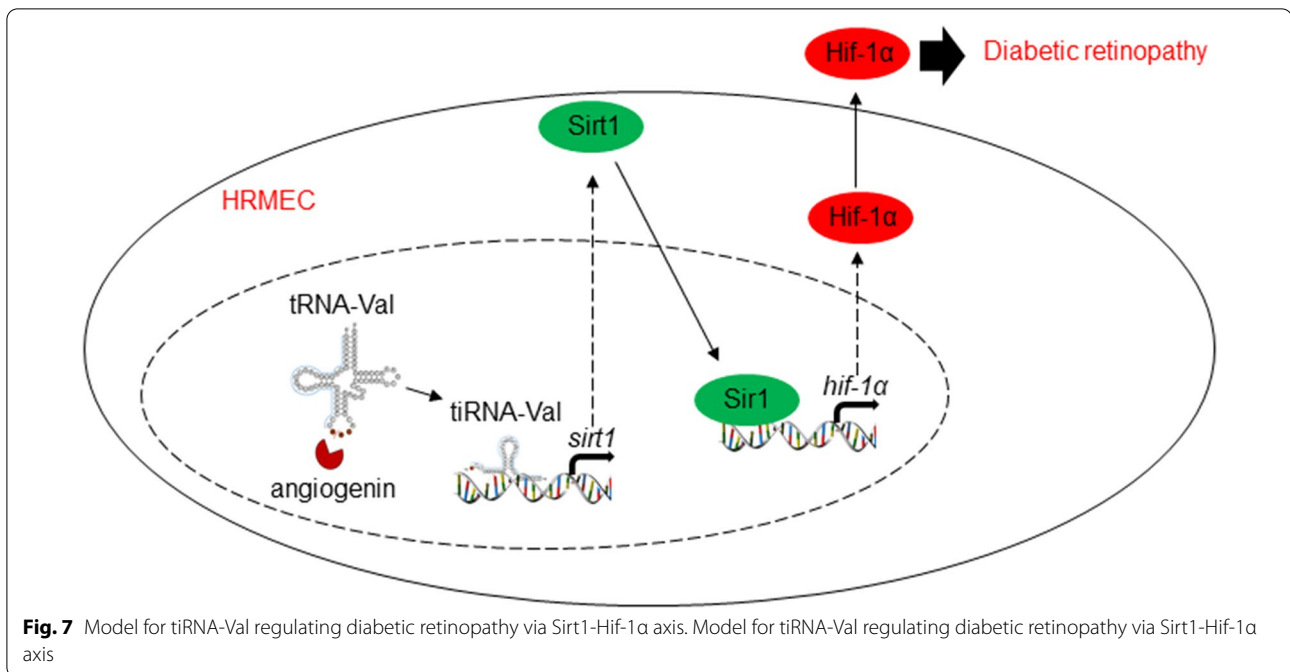
associated with DR progression, such as apoptosis and proliferation [28]. Here, we found that Sirt1 was down-regulated by tiRNA-Val, leading to the accumulation of Hif-1 α in HRMECs. Meanwhile, the knockdown of tiRNA-Val with shtiRNA-Val AAV subretinal injection ameliorates DR via Sirt1-Hif-1 α axis in vivo.

In summary, we identified and characterized a small RNA, tiRNA-Val, that regulates diabetic retinopathy

by modulating cell proliferation, and we have shown a potential approach that can be used to improve diabetic retinopathy by knocking down tiRNA-Val.

Conclusions

Our data manifested that Sirt1 was downregulated by tiRNA-Val, leading to the accumulation of Hif-1 α in HRMECs. Meanwhile, the knockdown of tiRNA-Val



with shtiRNA-Val AAV subretinal injection ameliorates DR via Sirt1-Hif-1α axis in vivo..

Abbreviations

DR: Diabetic retinopathy; tiRNAs: TRNA-derived stress-induced RNAs; HRMEC: Human retinal microvascular endothelial cell; ncRNAs: Noncoding RNAs.

Supplementary Information

The online version contains supplementary material available at <https://doi.org/10.1186/s40659-022-00381-7>.

Additional file 1. Supplementary figures. **(a)** 1% agarose gel electrophoresis were used to the analysis RNA integrity and the sample with 28S/18S = 1.5–2.0 were chosen for the following research. DR: diabetic retinopathy. **(b)** From the Northern result of tRNA-Val, we did not find the difference of precursor tRNA. Precursor tRNA containing 5' leader sequence, 3' trailer sequence and intron was not considered in this study. High, high glucose.

Additional file 2. Supporting Information Table. **Table S1.** Primers for mRNA detection by RT-qPCR. **Table S2.** Sequences of adapters and primers for tiRNA quantification by TaqMan qRT-PCR. **Table S3.** 3'-DIG-labelled oligonucleotides probes.

Acknowledgements

Thanks for all the contributors.

Authors' contributions

YX and XX conceived and designed the study. YX and XX performed the experiments and drafted the manuscript. HZ, QD, YLZ, CT and YYL helped to analyze the data. XX supervised the experiments and revised the manuscript. All authors read and approved the final manuscript.

Funding

This work was supported by the Chinese National Natural Science Foundation (Grant No. 81970846).

Availability of data and materials

The datasets used or analyzed during the current study are available from the corresponding author on reasonable request.

Declarations

Ethics approval and consent to participate

Animal experiments were carried out with the approval of the Committee of Shanghai Eye Disease Prevention and Control Center/Shanghai Eye Hospital.

Consent for publication

Not applicable.

Competing interests

The authors declare that they have no competing interests.

Author details

¹Shanghai Eye Diseases Prevention & Treatment Center/ Shanghai Eye Hospital, Shanghai, China. ²Shanghai General Hospital, Shanghai, China. ³Shanghai Key Laboratory of Ocular Fundus Diseases, Shanghai, China. ⁴Shanghai Engineering Center for Visual Science and Photomedicine, Shanghai, China. ⁵Shanghai Engineering Research Center of Precise Diagnosis and Treatment of Eye Diseases, Shanghai, China (Project No. 19DZ2250100), Shanghai, China.

Received: 16 October 2021 Accepted: 22 February 2022

Published online: 26 March 2022

References

- Antonetti DA, Klein R, Gardner TW. Diabetic retinopathy. *N Engl J Med*. 2012;366(13):1227–39.
- Wong TY, Sabanayagam C. Strategies to tackle the global burden of diabetic retinopathy: from epidemiology to artificial intelligence. *Ophthalmologica*. 2020;243(1):9–20.
- Cheung N, Mitchell P, Wong TY. Diabetic retinopathy. *Lancet*. 2010;376(9735):124–36.
- Giacco F, Brownlee M. Oxidative stress and diabetic complications. *Circ Res*. 2010;107(9):1058–70.

5. Huang H, He J, Johnson D, Wei Y, Liu Y, Wang S, et al. Deletion of placental growth factor prevents diabetic retinopathy and is associated with Akt activation and HIF1alpha-VEGF pathway inhibition. *Diabetes*. 2015;64(1):200–12.
6. Antonetti DA, Barber AJ, Hollinger LA, Wolpert EB, Gardner TW. Vascular endothelial growth factor induces rapid phosphorylation of tight junction proteins occludin and zonula occluden 1. A potential mechanism for vascular permeability in diabetic retinopathy and tumors. *J Biol Chem*. 1999;274(33):23463–7.
7. Miyamoto K, Khosrof S, Bursell SE, Rohan R, Murata T, Clermont AC, et al. Prevention of leukostasis and vascular leakage in streptozotocin-induced diabetic retinopathy via intercellular adhesion molecule-1 inhibition. *Proc Natl Acad Sci USA*. 1999;96(19):10836–41.
8. Stachurska A, Zorro MM, van der Sijde MR, Withoff S. Small and long regulatory RNAs in the immune system and immune diseases. *Front Immunol*. 2014;5:513.
9. Yan B, Yao J, Liu JY, Li XM, Wang XQ, Li YJ, et al. lncRNA-MIAT regulates microvascular dysfunction by functioning as a competing endogenous RNA. *Circ Res*. 2015;116(7):1143–56.
10. Bao XY, Cao J. MiRNA-138-5p protects the early diabetic retinopathy by regulating NOVA1. *Eur Rev Med Pharmacol Sci*. 2019;23(18):7749–56.
11. Lee YS, Shibata Y, Malhotra A, Dutta A. A novel class of small RNAs: tRNA-derived RNA fragments (tRFs). *Genes Dev*. 2009;23(22):2639–49.
12. Peng H, Shi J, Zhang Y, Zhang H, Liao S, Li W, et al. A novel class of tRNA-derived small RNAs extremely enriched in mature mouse sperm. *Cell Res*. 2012;22(11):1609–12.
13. Honda S, Loher P, Shigematsu M, Palazzo JP, Suzuki R, Imoto I, et al. Sex hormone-dependent tRNA halves enhance cell proliferation in breast and prostate cancers. *Proc Natl Acad Sci USA*. 2015;112(29):E3816–25.
14. Kumar P, Kusc C, Dutta A. Biogenesis and Function of Transfer RNA-Related Fragments (tRFs). *Trends Biochem Sci*. 2016;41(8):679–89.
15. Kim HK. Transfer RNA-derived small non-coding RNA: dual regulator of protein synthesis. *Mol Cells*. 2019;42(10):687–92.
16. Gebetsberger J, Wyss L, Mleczo AM, Reuther J, Polacek N. A tRNA-derived fragment competes with mRNA for ribosome binding and regulates translation during stress. *RNA Biol*. 2017;14(10):1364–73.
17. Goodarzi H, Liu X, Nguyen HC, Zhang S, Fish L, Tavazoie SF. Endogenous tRNA-derived fragments suppress breast cancer progression via YBX1 displacement. *Cell*. 2015;161(4):790–802.
18. Kim HK, Fuchs G, Wang S, Wei W, Zhang Y, Park H, et al. A transfer-RNA-derived small RNA regulates ribosome biogenesis. *Nature*. 2017;552(7683):57–62.
19. Rakoczy PE, Brankov M, Fonceca A, Zaknich T, Rae BC, Lai CM. Enhanced recombinant adeno-associated virus-mediated vascular endothelial growth factor expression in the adult mouse retina: a potential model for diabetic retinopathy. *Diabetes*. 2003;52(3):857–63.
20. Fu H, Feng J, Liu Q, Sun F, Tie Y, Zhu J, et al. Stress induces tRNA cleavage by angiogenin in mammalian cells. *FEBS Lett*. 2009;583(2):437–42.
21. Zhang Y, Zhang X, Shi J, Tuorto F, Li X, Liu Y, et al. Dnmt2 mediates intergenerational transmission of paternally acquired metabolic disorders through sperm small non-coding RNAs. *Nat Cell Biol*. 2018;20(5):535–40.
22. Bapputty R, Talahalli R, Zarini S, Samuels I, Murphy R, Gubitosi-Klug R. Montelukast prevents early diabetic retinopathy in mice. *Diabetes*. 2019;68(10):2004–15.
23. Wang AL, Rao VR, Chen JJ, Lussier YA, Rehman J, Huang Y, et al. Role of FAM18B in diabetic retinopathy. *Mol Vis*. 2014;20:1146–59.
24. Barot M, Gokulgandhi MR, Patel S, Mitra AK. Microvascular complications and diabetic retinopathy: recent advances and future implications. *Future Med Chem*. 2013;5(3):301–14.
25. Ivanov P, Emara MM, Villen J, Gygi SP, Anderson P. Angiogenin-induced tRNA fragments inhibit translation initiation. *Mol Cell*. 2011;43(4):613–23.
26. Lin M, Chen Y, Jin J, Hu Y, Zhou KK, Zhu M, et al. Ischaemia-induced retinal neovascularisation and diabetic retinopathy in mice with conditional knockout of hypoxia-inducible factor-1 in retinal Muller cells. *Diabetologia*. 2011;54(6):1554–66.
27. Li HY, Yuan Y, Fu YH, Wang Y, Gao XY. Hypoxia-inducible factor-1alpha: A promising therapeutic target for vasculopathy in diabetic retinopathy. *Pharmacol Res*. 2020;159:104924.
28. Ryu DR, Yu MR, Kong KH, Kim H, Kwon SH, Jeon JS, et al. Sirt1-hypoxia-inducible factor-1alpha interaction is a key mediator of tubulointerstitial damage in the aged kidney. *Aging Cell*. 2019;18(2):e12904.
29. Raina M, Ibba M. tRNAs as regulators of biological processes. *Front Genet*. 2014;5:171.
30. Thompson DM, Parker R. Stressing out over tRNA cleavage. *Cell*. 2009;138(2):215–9.
31. Saikia M, Jobava R, Parisien M, Putnam A, Krokowski D, Gao XH, et al. Angiogenin-cleaved tRNA halves interact with cytochrome c, protecting cells from apoptosis during osmotic stress. *Mol Cell Biol*. 2014;34(13):2450–63.
32. Chen Q, Yan M, Cao Z, Li X, Zhang Y, Shi J, et al. Sperm tsRNAs contribute to intergenerational inheritance of an acquired metabolic disorder. *Science*. 2016;351(6271):397–400.
33. Maute RL, Schneider C, Sumazin P, Holmes A, Califano A, Basso K, et al. tRNA-derived microRNA modulates proliferation and the DNA damage response and is down-regulated in B cell lymphoma. *Proc Natl Acad Sci USA*. 2013;110(4):1404–9.
34. Lalaouna D, Carrier MC, Semsey S, Brouard JS, Wang J, Wade JT, et al. A 3' external transcribed spacer in a tRNA transcript acts as a sponge for small RNAs to prevent transcriptional noise. *Mol Cell*. 2015;58(3):393–405.
35. Karbasforooshan H, Karimi G. The role of SIRT1 in diabetic retinopathy. *Biomed Pharmacother*. 2018;97:190–4.
36. Mishra M, Duraisamy AJ, Kowluru RA. Sirt1: a guardian of the development of diabetic retinopathy. *Diabetes*. 2018;67(4):745–54.

Publisher's Note

Springer Nature remains neutral with regard to jurisdictional claims in published maps and institutional affiliations.

Ready to submit your research? Choose BMC and benefit from:

- fast, convenient online submission
- thorough peer review by experienced researchers in your field
- rapid publication on acceptance
- support for research data, including large and complex data types
- gold Open Access which fosters wider collaboration and increased citations
- maximum visibility for your research: over 100M website views per year

At BMC, research is always in progress.

Learn more biomedcentral.com/submissions

